XXXI Congresso Nacional de Estudantes de Engenharia Mecânica
29 de Setembro a 03 de Outubro de 2025, São Carlos - SP, Brasil

GUIDELINES FOR BANDWIDTH SELECTION FOR LEAK NOISE DETECTION IN BURIED PIPELINES

Letícia Caroline dos Santos Assis, lcs.assis@unesp.br[1]
Oscar Scussel, oscar.scussel@unesp.br[2]

[1]São Paulo State University, UNESP-FEIS, Department of Mechanical Engineering, 15385-007, Ilha Solteira-SP, Brazil.

Resumo. *A detecção precisa de vazamentos em tubulações de água enterradas continua sendo um desafio significativo, principalmente devido à dificuldade de prever a largura de banda de frequência do ruído do vazamento antes dos testes acústicos no local. Essa faixa de frequência é fundamental para configurar correladores acústicos e otimizar o posicionamento dos sensores, porém, atualmente não existe um método prático amplamente adotado para estimá-la antecipadamente. Este artigo revisa uma abordagem baseada em modelos para prever a largura de banda do ruído de vazamento e examina os principais fatores que a influenciam. Ao representar o sistema tubo–solo–sensor como uma série de filtros, o método explorado analisa como características físicas e geométricas afetam a propagação do sinal. São investigados dois modelos para a predição do número de onda da onda induzida pelo vazamento, considerando parâmetros chave como espaçamento entre sensores, velocidade de propagação e atenuação. As larguras de banda previstas são validadas com medições obtidas em um banco de ensaio experimental. Os resultados indicam que as propriedades do tubo e do solo, assim como o tipo de transdutor, são fatores dominantes na propagação do ruído do vazamento. Essas conclusões possibilitam estimativas mais precisas da largura de banda e contribuem para o desenvolvimento de estratégias aprimoradas de detecção de vazamentos.*

Palavras chave: *Banda de Frequência do Ruído de Vazamento, Tubulações Enterradas, Propagação de Ondas, Correlacionador Acústico*

Abstract. *Accurate leak detection in buried water pipelines remains a significant challenge, particularly due to the difficulty in predicting the frequency bandwidth of leak noise prior to on-site testing using acoustic methods. This frequency range is critical for configuring acoustic correlators and optimizing sensor deployment, yet no widely adopted practical method currently exists to estimate it in advance. This paper reviews a model-based approach that has been proposed to predict leak noise bandwidth and examines the key factors influencing it. By representing the pipe–soil–sensor system as a series of filters, the reviewed method explores how physical and geometric characteristics affect signal propagation. Two models for wavenumber prediction of the leak-induced wave are investigated, considering key parameters such as sensor spacing, wave speed, and attenuation. The predicted bandwidths are then validated using measurements from an experimental test rig. Results show that pipe and soil properties, as well as transducer type, are dominant factors influencing leak noise propagation. These findings support more accurate bandwidth estimation and improved leak detection strategies.*

Keywords: *Leak Noise Bandwidth, Buried Pipelines, Wave Propagation, Acoustic Correlator*

1. INTRODUCTION

Water loss from distribution systems due to leakage is a significant global issue, posing a major challenge for water utility companies (Hu et al., 2021; Waqar et al., 2025). Over the past few decades, various techniques have been developed to detect and locate these leaks, each with its own advantages and limitations (Gao et al, 2018; Liu et al., 2025). This paper focuses on one specific method: the use of a leak noise correlator. This device detects leak noise by measuring acoustic pressure or pipe vibrations on either side of a leak. The peak in the cross-correlation of these signals provides the time difference of arrival at the sensor positions, which, along with the distance between sensors and the wave speed of the leak noise, allows for determining the leak's location (Cui et al., 2023). As the leak noise propagates along the pipe, it is filtered by the pipe system and shaped by the frequency response characteristics of the sensors. Depending on the sensor type, this combination can act as a low-pass or band-pass filter (Brennan et al., 2018).

Recent studies have advanced models of the pipe system by considering the effects of surrounding soil, providing a more comprehensive understanding of leak noise propagation (Scussel et al., 2024). A critical aspect of leak detection is determining the bandwidth in which leak noise exists, as it varies depending on factors such as pipe type, sensor type, and location. Traditionally, this bandwidth has only been estimated through complex and time-consuming field measurements.

Scussel et al. (2023) addressed this challenge by introducing a technique based on a simplified analytical model that links physical characteristics of the pipe-soil-sensor system with the measurable bandwidth of leak noise. This paper reviews and builds upon that technique, providing a detailed examination of how key physical parameters, such as pipe geometry, soil type, and sensor characteristics, affect the cross-power spectral density (CPSD) of the signals and influence the effective bandwidth for leak detection using acoustic correlators.

This paper is organized as follows. Following this introduction, Section 2 introduces the analytical models used to predict the wavenumber of fluid-borne leak noise waves propagating in buried, fluid-filled plastic pipes. Section 3 provides an overview of the factors affecting the leak noise wave bandwidth in such pipelines. Section 4 presents some experimental work and analysis. Some conclusions are then given in Section 5.

2. ANALYTICAL MODELS FOR LEAK NOISE WAVENUMBER PREDICTION

This section introduces two analytical models used to predict axisymmetric wave propagation in buried, fluid-filled plastic pipes under varying pipe-soil coupling conditions. At frequencies below the pipe's ring frequency, the dominant axisymmetric ($n = 0$) and fluid-driven ($s = 1$) wavenumber behavior has been explored under two key coupling scenarios: (1) the no-slip condition, where the pipe-soil interface is in full contact (compact coupling), and (2) the slip condition, where the interface is assumed to be lubricated, partial or frictionless contact, as investigated by Brennan et al. (2018) and Scussel et al. (2024). Figure 1 shows a typical water leak problem using vibro-acoustic correlators.

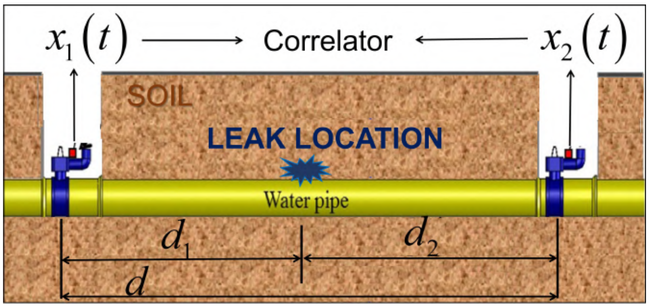

Figure 1. Typical water leak detectionn problem using acoutic correlator

In order to aid physical insight, they can be rewritten in terms of dynamic stiffnesses as follows

$$k = k_{\text{water}} \left(1 + \frac{K_{\text{water}}}{K_{\text{pipe}} + K_{\text{soil}}}\right)^{\frac{1}{2}} \tag{1}$$

where $k_{\text{water}} = \omega(\rho_{\text{water}}/B_{\text{water}})^{\frac{1}{2}}$ is the free-field wavenumber of water, which is a function of the density ρ_{water} the corresponding bulk modulus B_{water} and the angular frequency ω. The term $K_{\text{water}} = 2B_{water}/a$ is the stiffness of the water and

$$K_{\text{pipe}} = \frac{K_{\text{pipe}}^{(\text{stiff})}}{(1-\nu_p^2)} + K_{\text{pipe}}^{(\text{inertia})} = \frac{E_p^* h}{a^2(1-\nu_p^2)} - \omega^2 \rho_p h \tag{2}$$

is the stiffness of the pipe-wall where a is the mean radius, h is the thickness, ρ_p, $E_p^* = E_p(1 + j\eta_p)$ and ν_p are the density, Young's modulus and Poisson's ratio of the pipe, respectively. The term η_p is the loss factor of the pipe.

The term $K_{\text{pipe}}^{(\text{stiff})}$ denotes the stiffness component of pipe-wall and $K_{\text{pipe}}^{(\text{inertia})}$ corresponds to the inertial component. Additionally, the term K_{soil} in Eq. (1) denotes the stiffness of the surrounding soil. Note that the soil properties affect drastically the propagation characteristics of the fluid-borne $s = 1$ wave travelling on the pipe since part of its energy propagates into the soil. Thus, two different boundary conditions at the pipe-soil interface are considered: one that assumes the pipe-soil interaction under lubricated contact (slip coupling) where there is no frictional stress applied on the axial direction, and the other one that assumes the pipe-soil interaction under compact contact (no-slip coupling) with propagation on both axial and radial directions.

The soil dynamic stiffness for the slip coupling condition can be written as a combination of three components, so the term K_{soil} in Eq. (1) becomes (Brennan et al., 2018):

$$K_{\text{soil}}^{\text{slip}} = K_1 + K_2 + K_3 \tag{3}$$

in which

$$K_1 = \left(B_s^* - \frac{2G_s^*}{3}\right) \frac{k_d^2}{k_d^r} \left(1 - 2\frac{k^2}{k_r^2}\right) \frac{H_0\left(k_d^r a\right)}{H_0'\left(k_d^r a\right)} \tag{4}$$

$$K_2 = -2G_s^* k_d^r \left(1 - 2\frac{k^2}{k_r^2}\right) \frac{H_1'(k_d^r a)}{H_1(k_d^r a)} \tag{5}$$

$$K_3 = -4G_s^* k_r^r \frac{k^2}{k_r^2} \frac{H_1'(k_r^r a)}{H_1(k_r^r a)} \tag{6}$$

For the no-slip coupling condition, the soil dynamic stiffness term K_{soil} in Eq. (1) becomes

$$K_{\text{soil}}^{\text{noslip}} = \frac{\mu_s}{a} K_a + \frac{E_p^* h}{a^2(1-\nu_p^2)} K_b \tag{7}$$

where

$$K_a = 2 + \frac{k_r^r a k_r^2 a^2 \left[\frac{H_0(k_r^r a)}{H_0'(k_r^r a)}\right]\left[\frac{H_0(k_d^r a)}{H_0'(k_d^r a)}\right]}{k_r^r a k_d^r a \left[\frac{H_0(k_r^r a)}{H_0'(k_r^r a)}\right] + k^2 a^2 \left[\frac{H_0(k_d^r a)}{H_0'(k_d^r a)}\right]} \tag{8}$$

$$K_b = -\frac{\nu_p^2}{\left(1 + \frac{S_1}{k^2 a^2}\right)} + \frac{j2\nu_p S_2}{ka\left(1 + \frac{S_1}{k^2 a^2}\right)} + \frac{S_2^2}{k^2 a^2 \left(1 + \frac{S_1}{k^2 a^2}\right)} \tag{9}$$

in which

$$S_1 = -\mu_s \frac{(1-\nu_p^2)a}{E_p h} \left[\frac{k_d^r a k_r^2 a^2}{k_r^r a^2 k_d^r \left[\frac{H_0(k_r^r a)}{H_0'(k_r^r a)}\right] + k^2 a^2 \left[\frac{H_0(k_d^r a)}{H_0'(k_d^r a)}\right]}\right] \tag{10}$$

$$S_2 = \frac{j\mu_s(1-\nu_p^2)ka^2}{E_p h} \left[2 - \frac{k_r^2 a^2 \left[\frac{H_0(k_d^r a)}{H_0'(k_d^r a)}\right]}{k_r^r a^2 k_d^r \left[\frac{H_0(k_r^r a)}{H_0'(k_r^r a)}\right] + k^2 a^2 \left[\frac{H_0(k_d^r a)}{H_0'(k_d^r a)}\right]}\right] \tag{11}$$

Moreover, the soil radial wavenumbers k_d^r and k_r^r, are given by $k_d^r = \sqrt{k_d^2 - k^2}$ and $k_r^r = \sqrt{k_r^2 - k^2}$ where k_d and k_r are the compressional and shear wavenumbers in the surrounding soil, respectively, given by $k_d^2 = \omega^2 \rho_s/(\lambda_s + 2\mu_s)$ and $k_r^2 = \omega^2\rho_s/\mu_s$ in which ρ_s is the soil density and $\lambda_s = B_s^* - \frac{2}{3}G_s^*, \mu_s = G_s^*$ are the Lamé coefficients, which are function of bulk modulus $B_s^* = B_s(1 + j\eta_{\text{soil}})$ and shear modulus $G_s^* = G_s(1 + j\eta_{\text{soil}})$ of the soil. The terms H_0, H_1 are the Hankel functions of zero, first order and second kind, respectively, that describe the outgoing waves in the surrounding soil, and $'$ denotes the spatial derivative.

The attenuation of the fluid-borne wave in terms of dB/m is given by (Brennan et al., 2018):

$$\text{Attenuation} = \frac{-20\text{Im}\{k\}}{\ln(10)} \tag{12}$$

For a fluid-filled pipe in-air there is no surrounding soil present in the model, so that $K_{\text{soil}} = 0$.

3. EXPLORING THE FACTORS AFFECTING THE BANDWIDTH OF MEASURED LEAK NOISE WAVE

An alternative way to represent a typical water leak detection problem is by modeling each component in the system as a filter, resulting in a cascade of filters. These include filters associated with the water-filled pipe stiffness, the pipe's mass, the surrounding medium, time delay due to wave propagation, and the transducer dynamics (e.g., accelerometers). Among these, the transducer, the pipe, and the surrounding medium have the most significant influence on the bandwidth of the measured leak noise (Scussel et al., 2023). The filtering effects of each component and their combinations have been analyzed in terms of the modulus of the Cross Power Spectral Density (CPSD), revealing the frequency-dependent behavior of leak noise transmission. A key outcome of this analysis is the identification of the bandwidth of the complete system, comprising the pipe, surrounding medium, and accelerometers, as the frequency range in which the modulus of the CPSD remains within 10 dB of its maximum. Detailed results for different soil types and system configurations are given in Fig. 2 and more details can be found in Scussel et al. (2023). Note that the vertical dashed green lines denote the upper and lower frequencies estimated by the algorithm which varies according to the surrouding medium.

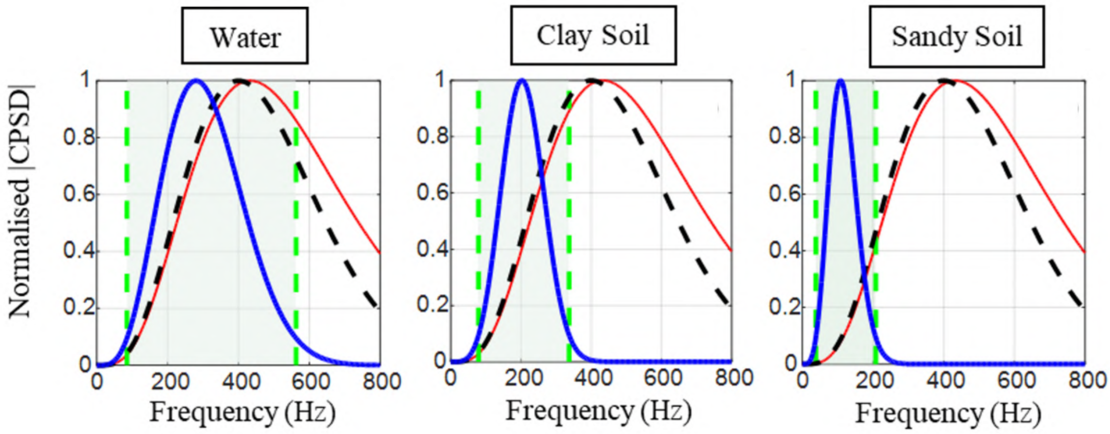

Figure 2. Behaviour of the water pipe system modelled as a set of filters connected in series. Continous thin red line is the mass-less-in-vacuo pipe, dashed black line invoes addtion of intertial effects and the continuos thick blue line further involves the external medium

4. EXPERIMENTAL WORK AND DISCUSSION

The aim of this study is to evaluate the influence of the pipe-soil interface - in compact and lubricated contact - on the propagation of the axisymmetric acoustic wave (s = 1) in plastic pipes filled with water, based on data from the Blithfield test rig in the UK. The following results were obtained from signals measured in a medium-density polyethylene (MDPE) pipe, considering known distances between sensors and between the point of leakage and the sensors, these distances can be seen in Tab.1. The properties of the pipe system in the case studied are shown in Tab.2.

Table 1. Distances between leak and sensor positions

Parameter	Value	Unit
Distance between leak and P1 d_1	0	m
Distance between leak and P2 d_2	30	m
Distance between access points d	30	m
Distance difference Δd	30	m

Table 2. Material and geometric properties of the MDPE pipe

Property	Value	Unit
Young's Modulus E	2×10^9	N/m^2
Loss Factor η_p	0.06	–
Density ρ	900	kg/m^3
Poisson's Ratio ν	0.4	–
Outer Radius a	0.08000	m
Wall Thickness h	0.00985	m

Figure 3 shows a comparison between the real part of the wave number, wave attenuation and wave speed, between the models in air, lubricated contact, compact contact and experimental.

Analyzing the real part behaviour of the wavenumber, it indicates good agreement between the predicted and measured data from the Blithfield test rig, with only minor discrepancies observed at lower and higher frequencies.

While the real part of the wavenumber exhibits similar trends across models, notable differences arise in wave speed and attenuation. Wave speed, calculated from the real part of the wave number, varies among the models. The compact model exhibits a higher and more variable wave speed (390–410 m/s) within the relevant frequency range. In contrast, the lubricated model shows a lower but more consistent speed (374-381 m/s). The in-air model presents a constant wave speed, as its parameters are frequency-independent. These differences are primarily attributed to variations in soil shear stiffness.

In the compact model, the strong coupling between the soil and the pipe increases the effective stiffness, resulting in higher wave speed. Conversely, the lubricated model's weaker coupling leads to reduced wave propagation speed.

Attenuation behavior also differs across models. The compact model shows higher attenuation, while the lubricated model exhibits lower attenuation that increases more gradually with frequency. This attenuation arises from both internal material damping in the pipe and radiation losses into the surrounding ground.

For the in-air model, attenuation remains low and increases gradually, as there is no energy radiation to the surrounding environment, unlike in buried conditions. Across all three models, the experimental data align most closely with the compact model, indicating it provides the best representation of the physical system.

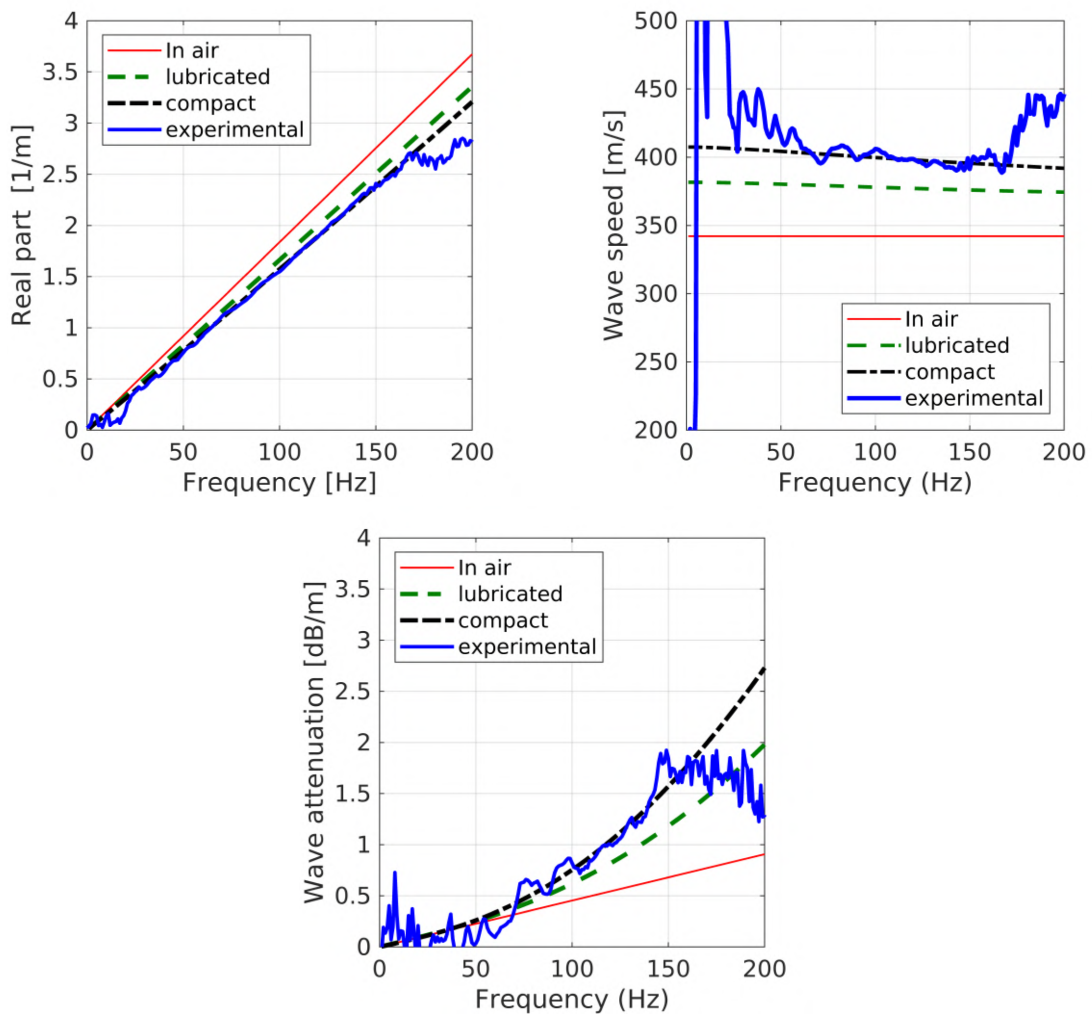

Figure 3. Wavenumber, wave attenuation and wave speed: Comparison of the analytical models, in air, lubricated and compatc contacts, along with experimental results

The coherence between the signals provides an indicator of the quality of the spectral data for wave number estimation. Figure 4 shows good coherence of around 0.8 in the 50 Hz to 120 Hz range. A sharp drop in coherence outside this range indicates noise interference, which can also indicate a good frequency range for filtering.

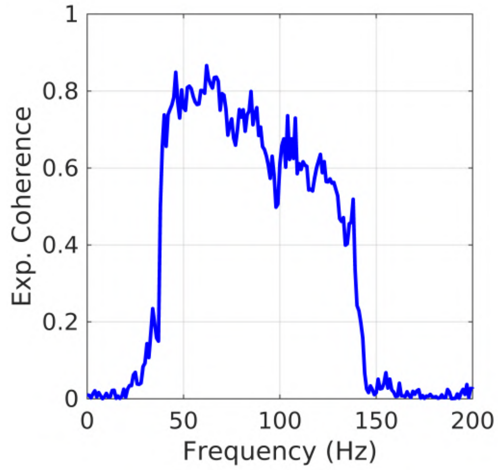

Figure 4. Coherence

Figure 5 compares the cross-power spectral density (CPSD) functions for the compact and lubricated contact models, based on the methodology described in Section 3. The effective frequency range for the lubricated model spans approximately 25–147 Hz, while for the compact model it is slightly narrower, around 22–123 Hz. This indicates that the compact contact configuration supports a narrower bandwidth for effective leak noise transmission compared to the lubricated model.

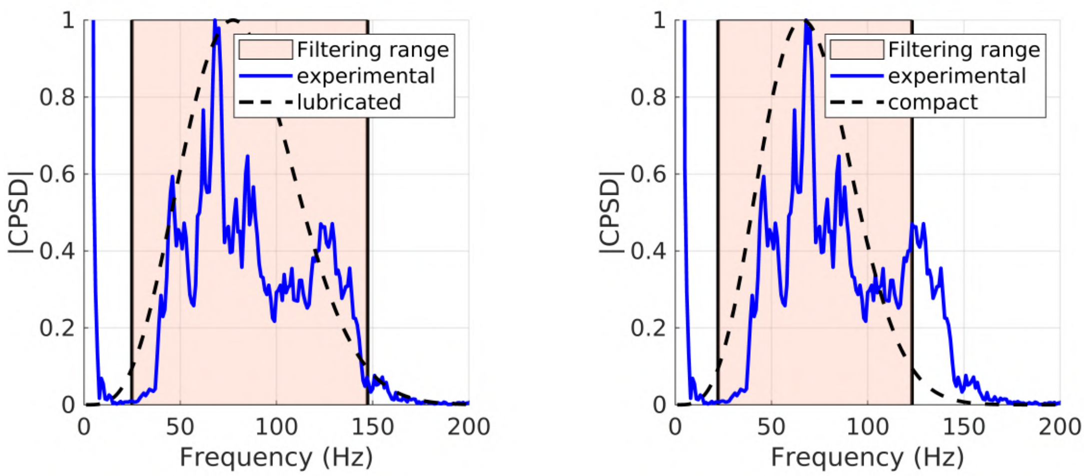

Figure 5. CPSD function for the leak noise wave bandwidth estimation using lubricated and compact contact models

5. FINAL REMARKS

This paper has investigated how the physical parameters of the water-pipe-soil-sensor system influence the bandwidth of measured leak noise. A simple analytical model of the pipe system, integrated with the sensor's frequency response, has been used to model the Cross Power Spectral Density (CPSD) between two sensors. The impact of various physical parameters on the CPSD and, consequently, the frequency bandwidth has been explored for three types of surrounding media: water, stiff clay soil, and sandy soil, using accelerometers as sensors. The results show that the surrounding medium significantly affects the frequency range in which leak noise is detected. Experimental analysis based on the Blithfield test rig data demonstrated good coherence between the measured signals and the model predictions, validating the proposed approach for representing the system's behavior.

6. ACKNOWLEDGEMENTS

This work was supported the São Paulo Research Foundation (FAPESP) under grant number 24/13559-0.

7. REFERENCES

Brennan, M.J., Karimi, M., Muggleton, J.M., de Almeida, F.C.L., de Lima, F.K., Ayala, P.C., Obata, D., Paschoalini, A.T., Kessissoglou, N., 2018. "On the effects of soil properties on leak noise propagation in plastic water distribution pipes". *J. Sound Vib.*, Vol. 427, p. 120–133.

Cui, X., Gao, Y., Ma, Y., Liu, F., Wang, H., 2023. "Time delay estimation using cascaded LMS filters fused by correlation coefficient for pipeline leak localization". *Mech. Syst. Signal Process.*, Vol. 199, p. 110500.

Gao, Y., Liu, Y., Ma, Y., Cheng, X., Yang, J., 2018. "Application of the differentiation process into the correlation-based leak detection in urban pipeline networks". *Mech. Syst. Signal Process.*, Vol. 112, p. 251–264.

Hu, Z., Tariq, S., Zayed, T., 2021. "A comprehensive review of acoustic based leak localization method in pressurized pipelines". *Mech. Syst. Signal Process.*, Vol. 161, p. 107994.

Liu, R., Zayed, T., Xiao, R., 2025. "Acoustic leak localization for water distribution network through time-delay-based deep learning approach". *Water Research*, Vol. 268 Part A, p. 122600.

Muggleton, J.M., Brennan, M.J., 2004. "Leak noise propagation and attenuation in submerged plastic water pipes". *J. Sound Vib.*, Vol. 278(3), p. 527–537.

Scussel, O., Brennan, M.J., de Almeida, F.C.L., Iwanaga, M.K., Muggleton, J.M., Joseph, P.F., Gao, Y., 2023. "Key factors that influence the frequency range of measured leak noise in buried plastic water pipes: Theory and experiment". *Acoust.*, Vol. 5, p. 490–508.

Scussel, O., Brennan, M.J., Muggleton, J.M., de Almeida, F.C.L., Joseph, P.F., Gao, Y., 2024. "An Investigation into the Physical Mechanisms of Leak Noise Propagation in Buried Plastic Water Pipes: A Wave Dynamic Stiffness Approach". *Acoust.*, Vol. 6(1), p. 157–176.

Waqar, M., Memon, A.M., Louati, M., Ghidaoui, M.S., Alhems, L.M., Meniconi, S., Brunone, B., Capponi, C., 2025. "Pipeline leak detection using hydraulic transients and domain-guided machine learning". *Mech. Syst. Signal Process.*, Vol. 224, p. 111967.

8. RESPONSIBILITY FOR THE INFORMATION

The authors are solely responsible for the information included in this work.